STABILITY RELATIONS OF RHODOCHROSITE IN THE SYSTEM MANGANESE-CARBON-OXYGEN[1]

J. Stephen Huebner, *U. S. Geological Survey, Washington, D. C. 20242.*

Abstract

The common occurrence of rhodochrosite with hausmannite (Mn_3O_4) and its rare equilibrium association with manganosite ($Mn_{1-x}O$), bixbyite (Mn_2O_3), and pyrolusite (MnO_2) are natural expressions of the f_{O_2}, f_{CO_2}, and temperature dependence of the rhodochrosite stability field. The relationships of those variables of the bounding reactions which produce manganese oxides and graphite were determined using rhodochrosite charges surrounded by oxygen buffers in a $CO_2 + CO$ atmosphere. The rhodochrosite-manganosite-gas equilibrium surface, determined on the graphite, Ni-NiO, and manganosite-hausmannite buffers at 1000, 1500, and 2000 atmospheres is given by the equation (°K, atm)

$$\log f_{CO_2} = 8.662 - \frac{5556}{T} - 0.0944\frac{p}{T} .$$

This equilibrium is independent of f_{O_2} within the limits of experimental error ($\pm 5°C$, ± 40 atm p_{CO_2}). The rhodochrosite-hausmannite-gas equilibrium constant, determined on the manganosite-hausmannite and hausmannite-bixbyite buffers, is given by the equation

$$\log K = 6 \log f_{CO_2} - \log f_{O_2} = 40.39 - \frac{9429}{T} + 0.486 \frac{p}{T} .$$

Experimental data for reactions between rhodochrosite and the manganese oxides, supplemented by thermodynamic calculations, indicate that at 1000 atmospheres the rhodochrosite field boundary decreases from $715° \pm 5°C, -12.5 \log f_{O_2}$ (atm.) units on the $Mn_{1-x}O$-Mn_3O_4 buffer, to $330° \pm 23°C, -8.4 \log f_{O_2}$ units on the Mn_3O_4-Mn_2O_3 buffer, and to $260° \pm 35°C, -5.6 \log f_{O_2}$ units on the Mn_2O_3-MnO_2 buffer. Rhodochrosite is stable at high temperatures only at low f_{O_2}. Comparison of the siderite, calcite, and magnesite stability fields with that of rhodochrosite suggests that the addition of manganese expands the siderite, reduces the calcite, and causes little change in the magnesite fields. Oxygen fugacities encountered in the MnO-C-O system are higher than those in corresponding iron-bearing systems. Metamorphic manganese oxide bodies have high inherited f_{O_2} values due to internal buffering, which causes gradients between such bodies and country rocks containing iron oxides or graphite.
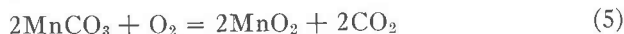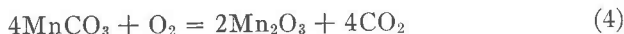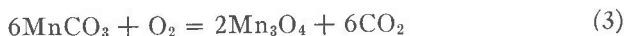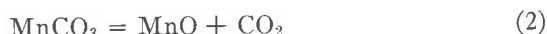
Introduction

Manganese is estimated to be the eleventh most abundant element in the earth's crust, but there have been few investigations of the behavior of manganese minerals under conditions approximating those of metamorphism. The present research concerns the phase relations of rhodochrosite ($MnCO_3$) with manganese oxides at moderate temperatures and pressures. By comparing the pressure (p)-temperature (T)-oxygen fugacity (f_{O_2}) conditions for carbonate-oxide equilibria of manganese with

---

[1] Publication authorized by the Director, U. S. Geological Survey.

those in similar systems containing iron, calcium, and magnesium, it is possible to predict the effect of the rhodochrosite component on the phase relations of manganiferous calcite, siderite, and magnesite. The geochemical behavior of manganese is most similar to that of iron. Differences in the oxidation potentials of iron and manganese, and in the solubilities of their compounds (Krauskopf, 1957), are perhaps best indicated by the effective separation of manganese from iron to form nearly pure sedimentary manganese oxide and carbonate deposits.

Because manganese has many oxidation states it forms various oxides approximately represented by the formulas MnO, Mn_3O_4, Mn_2O_3, and MnO_2. On a fugacity diagram the rhodochrosite stability field is bounded by five reactions:

$$MnCO_3 = MnO + C + O_2 \tag{1}$$

$$MnCO_3 = MnO + CO_2 \tag{2}$$

$$6MnCO_3 + O_2 = 2Mn_3O_4 + 6CO_2 \tag{3}$$

$$4MnCO_3 + O_2 = 2Mn_2O_3 + 4CO_2 \tag{4}$$

$$2MnCO_3 + O_2 = 2MnO_2 + 2CO_2 \tag{5}$$

All but reaction (2) involve an exchange of oxygen between the solid phases and vapor; carbon dioxide participates in all reactions but (1). Any experimental investigation of these reactions must include the evaluation of both the oxygen and the carbon dioxide fugacities.

CRYSTAL CHEMISTRY OF MINERALS IN THE SYSTEM Mn-C-O

Rhodochrosite commonly occurs as a component in rhombohedral carbonates and as a nearly pure end member mineral in sedimentary, metasedimentary, and hydrothermal ore bodies. Although the crystal structure has not been determined directly, rhodochrosite is placed with great certainty in the calcite group.

At moderate temperatures (above 450°C) and at pressures sufficient to prevent decomposition, rhodochrosite forms complete solid solutions with calcite (Goldsmith and Graf, 1957), siderite (Rosenberg, 1963), and magnesite (Goldsmith, 1960; Rosenberg, 1963). At lower temperatures there is an immiscibility gap between rhodochrosite and calcite (Goldsmith and Graf, 1957). Natural rhodochrosites show extensive solid solution with calcite and siderite, but contain little magnesium; many calcites, magnesites, and siderites contain small amounts of manganese.

The oxidation state of manganese in the carbonate structure is $+2$. The (104) interplanar spacings of ten synthetic rhodochrosite samples, equilibrated at varied conditions of temperature, pressure, and oxygen

fugacity (as discussed in this paper), were determined by averaging five or more X-ray powder diffractometer oscillations between the carbonate peak and either the silicon (111)[1] or NaCl (200) reflections. All synthetic rhodochrosite samples gave a (104) interplanar spacing of 2.844 ± 0.002 Å, internally consistent to ± 0.001 Å. Cell dimensions of three synthetic manganese carbonates were determined by refining 8 to 14 reflections with a computer program developed by Burnham (1962).[2] Agreement with results given by Graf (1961) and Swanson *et al.* (1957) is excellent.

Manganosite, $Mn_{1-x}O$, is such a rare mineral that it has been little investigated by geologists. Although manganosite forms complete solid solutions with CaO, MgO, and wustite at high temperatures (Jay and Andrews, 1945; Petterson, 1946; Foster and Welch, 1956; Glasser, 1962: and Riboud and Muan, 1962, 1963), natural manganosites are relatively pure (Palache *et al.*, 1944, p. 502). Several investigators have suggested that the oxygen content of manganosite varies in response to the oxygen fugacity (Le Blanc and Wehner, 1934; Rode, 1949; Moore *et al.*, 1950; Foster and Welch, 1956; Klingsberg and Roy, 1960; Davies and Richardson, 1959; Hed and Tannhauser, 1967; Schwerdtfeger and Muan, 1967), but the compositional limits are defined only between 1200° and 1650°C. Stoichiometric MnO has been prepared by Southard and Shomate (1942) and Rode (1949).

Hausmannite, Mn_3O_4, is a common mineral in metasedimentary manganese deposits. The mineral is tetragonal with a distorted spinel structure (Aminoff, 1926). Natural hausmannites contain less than 10 percent (weight) Fe_3O_4 and only small amounts of other cations. More iron-rich compositions on the join Mn_3O_4-Fe_3O_4 form intergrowths (vredenburgite) of hausmannite and jacobsite. Although the experimental investigations do not agree well, they suggest that limited substitution of iron in hausmannite is permitted at geologically reasonable temperatures (Mason, 1943; McMurdie *et al.*, 1950; Finch *et al.*, 1957; Van Hook and Keith, 1958; Ulrich *et al.*, 1966).

Natural bixbyite, Mn_2O_3, contains appreciable Fe_2O_3. The manganese end member α-Mn_2O_3 has been called "partridgeite" (Mason, 1944). Until recently α-Mn_2O_3 was assumed to be cubic, but Geller *et ai.* (1967) suggest that pure α-Mn_2O_3 may be orthorhombic at low temperatures. It is probable that α-Mn_2O_3 exists only as a stoichiometric oxide; Rode (1949) and Moore (1950) report the composition $MnO_{1.50}$. The composi-

[1] The unit-cell edge of silicon was taken to be 5.4306 Å.

[2] The average values of a, c, and V at 23°C are 4.7771₄ Å, 15.6628 Å, and 309.55 Å³, respectively. Standard deviations (one) of these three values are 0.00015, 0.0041 Å, and 0.08 Å³. Average absolute deviations of the three values are 0.00011, 0.0031 Å, and 0.064 Å³.

tion α-$MnO_{1.57}$ given by Le Blanc and Wehner (1934) is suspect because the sample may not have been homogeneous.

Tetragonal γ-Mn_2O_3 has a cation-deficient structure and variable composition (Verwey and de Boer, 1936; Moore *et al.*, 1950; O. P. Bricker, oral communication, 1966). Feitknecht (1964) and Oswald and Wampetich (1967) report a Mn_5O_8 phase formed as an intermediate step in the oxidation of small hausmannite grains. The X-ray powder diffraction patterns of hausmannite and γ-Mn_2O_3 are indistinguishable (see Bricker, 1965), but the reddish to cinnamon brown color of material encountered in this investigation is indicative of hausmannite. Pyrolusite is the only form of MnO_2 observed in this investigation.

EXPERIMENTAL INVESTIGATION

Previous work

The only previous experimental investigation of a reaction bounding the rhodochrosite stability field is a study of the decomposition of rhodochrosite to manganosite in an unbuffered carbon dioxide atmosphere by Goldsmith and Graf (1957). In order to prevent oxidation of the manganese these investigators evacuated their apparatus before admitting carbon dioxide; no attempt was made to determine or buffer the f_{O_2} of the system.

The equilibrium of siderite, the iron carbonate, with magnetite, graphite, and vapor, using sealed gold capsules, was investigated as a function of temperature and total pressure by Weidner and Tuttle (1965) and by Rosenberg (reported in French and Rosenberg, 1965). French (1964) determined the conditions of siderite decomposition along the graphite and magnetite-hematite buffers using open capsules and a $CO_2 + CO$ atmosphere. His results are in excellent agreement with those of Rosenberg but not those of Weidner and Tuttle.

Experimental procedure

The experimental procedure is largely patterned after that developed by French (1964). A synthetic, powdered $MnCO_3$ charge is placed in a small silver tube and the ends are loosely crimped. A larger silver tube with crimped ends encloses the appropriate buffer assemblage, which surrounds the charge capsule. With the Ni-NiO buffer, two concentric rhodochrosite charges are used to prevent contamination of the inner charge. Pressurized carbon dioxide passes through the crimped ends of the outer capsule and equilibrates with the buffer, fixing f_{O_2}, f_{CO}, and f_{CO_2}. This fluid equilibrates with the charge.

Standard hydrothermal bombs, modified from those described by Tuttle (1948, 1949), contained the charge and buffer assembly. Controllers maintained horizontal furnace temperatures to within $\pm 3°C$. The uncertainty in charge temperature measurement at any instant is estimated to be $\pm 2°C$. At any time during the run, charge temperatures are within $\pm 5°$ of the stated values. Total pressure (p) equalled the pressure of carbon dioxide supplied to the bomb. Bombs were open to a CO_2 line maintained within ± 15 atm of a constant value. Stated line pressure is accurate to ± 40 atm. Quenching was accomplished by closing the valve to the CO_2 line and placing the bomb in a jet of air for three minutes. Several initial runs were quenched in water.

The rhodochrosite charge material is Baker Analyzed Reagent Grade manganese carbonate, Lot No. 25699. As supplied by the manufacturer, the material is pale grayish brown (presumably slightly oxidized) and gives broad X-ray powder diffraction reflections.

Annealing for several hours within the rhodochrosite field causes the carbonate to become creamy white and the X-ray peaks to sharpen (see Goldsmith and Graf, 1957; Graf, 1961). Bixbyite and hausmannite were prepared by the thermal decomposition of polycrystalline pyrolusite, with tesserae exceeding 20 μm (Baker Analyzed MnO_2, Lot No. 22587) in a muffle oven at temperatures of approximately 800° and 1000°C, respectively. Manganosite was prepared from MnO_2 in a hydrogen atmosphere at 600°–700°C.

Determination of reaction

The double capsule arrangement with buffer surrounding charge enables both reactant and product to be used as starting materials in a single run. Outside the rhodochrosite field, the carbonate charge decomposes to oxide, commonly the lower oxide of the buffer pair. Rhodochrosite stability is indicated by the growth of carbonate rims around the buffer grains (Fig. 1). Minute amounts of highly anisotropic carbonate could be detected optically.

At high temperatures and within the rhodochrosite field, carbonate grows rapidly from manganosite and vapor. In several runs made outside the rhodochrosite field, carbonate formed during the quench. Charges and buffers were examined carefully to determine the extent of the reaction during quenching by X-ray diffraction methods and less frequently, optical techniques. Quench carbonate never exceeded more than several percent of the charge in contrast to the much higher percentage yields in runs demonstrating rhodochrosite formation.

Examination under incident light reveals partial reduction of initially homogeneous buffer grains during runs. Some bixbyite grains developed hausmannite rims (Fig. 2). Re-
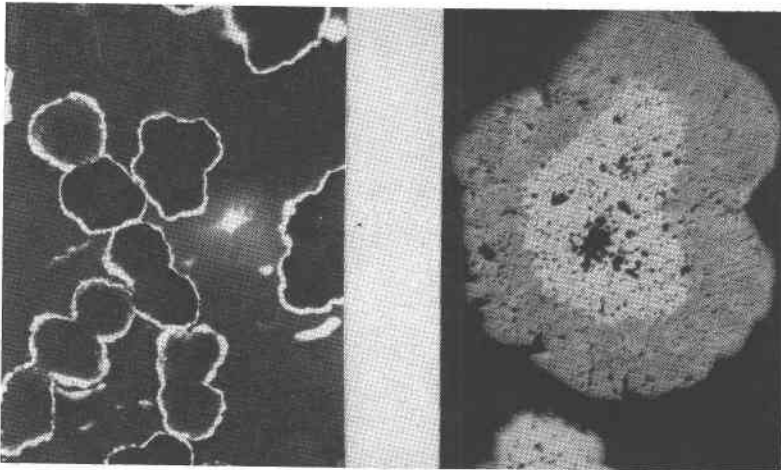

Fig. 1   Fig. 2

Fig. 1. Anisotropic rhodochrosite rims surround manganosite (translucent) and hausmannite (opaque) buffer grains, indicating the stability of carbonate at 701°C, $p_{co_2}+p_{co}=960$ atm, run of 94 hours duration. Oxide grains measure 0.1–0.2 mm. Crossed nicols.

Fig. 2. Bixbyite (Mn_2O_3) buffer grain marginally reduced to hausmannite (Mn_3O_4). Buffer originally consisted of homogeneous bixbyite (lighter gray) and hausmannite (darker gray) grains. Grain 0.2 mm long. Nonpolarized, reflected light.

duction of bixbyite also occurs along cracks and grain boundaries but cannot be adequately photographed. Some grains show no sign of reduction.

Oxygen fugacity-temperature relations of oxygen buffer curves

Buffer curves pertinent to the present study have been brought together in Figure 3 The log f_{O_2} *vs* reciprocal absolute temperature curve of the graphite-vapor buffer is from French and Eugster (1965) who calculated the equilibrium fugacities from thermodynamic data. The curve for the Ni-NiO buffer is given by Eugster and Wones (1962) and has been validated by Huebner and Sato (1968).

The manganosite-hausmannite buffer has been used by Lindsley (1963), Ernst (1966), and Gilbert (1966). These investigators extrapolated the equation of Hahn and Muan (1960) to lower temperatures but did not consider the cubic to tetragonal transition of Mn_3O_4. Curves based on thermochemical data (Mah, 1960; Kubaschewski and Evans, 1958) and several other experimental methods (Hahn and Muan, 1960; Blumenthal and Whitmore, 1961; Isihara and Kigoshi, 1953; Kim *et al.*, 1966; Hochgeschwender and Ingraham, 1967; Schwerdtfeger and Muan, 1967; Huebner and Sato, 1968) disagree with each other.

For this study, the manganosite-hausmannite buffer curve selected is given by Huebner and Sato (1968), whose results are in agreement with those of Hahn and Muan (1960),
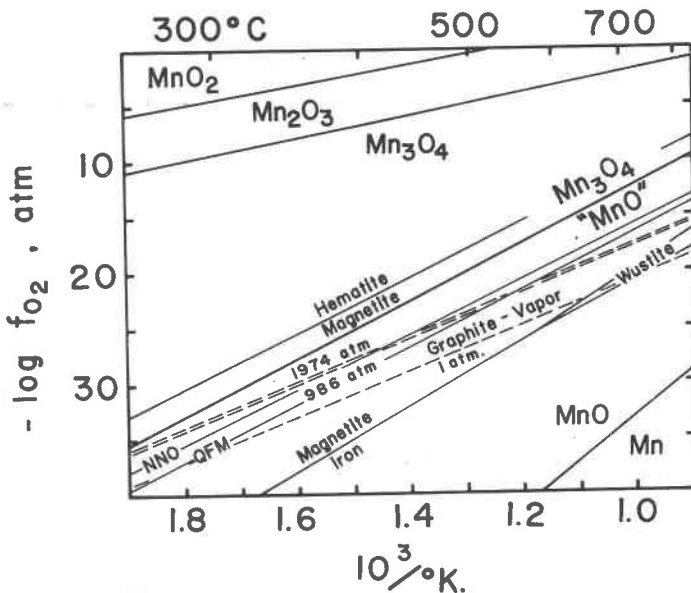

Fig. 3. Mn-O, Fe-O, and C-O system buffers in an f_{O_2}-t diagram. Unless otherwise shown, the change in oxygen fugacity as pressure changes from 1 to 2000 atm is too small to be seen on this diagram. Source of data: Mn-"MnO" (Mah, 1960); "MnO"-Mn_3O_4 (Huebner and Sato, 1968); Mn_3O_4-Mn_2O_3 (Huebner and Sato, 1968); Mn_2O_3-MnO_2 (Mah, 1960); Fe-Fe_3O_4 (Eugster and Wones, 1962); Fe-FeO (Eugster and Wones, 1962); FeO-Fe_3O_4 (Eugster and Wones, 1962); Fe_3O_4-Fe_2O_3 (Eugster and Wones, 1962); Fe_2SiO_4-Fe_3O_4-SiO_2 (QFM) (D. R. Wones and C. Gilbert, oral communication, 1968); Graphite-vapor (French and Eugster, 1965); Ni-NiO (NNO) (Eugster and Wones, 1962; Huebner and Sato, 1968).

Schwerdtfeger and Muan (1967), and Hed and Tannhauser (1967). Molar volume data of Robie *et al.* (1966) and new unpublished data (Huebner and M. Sato) were used in calculating the total pressure-dependent correction term, $+0.0807$ ($p/T^\circ K$).

The hausmannite-bixbyite buffer has been determined by Huebner and Sato (1968). For total pressures other than one atmosphere, the pressure correction term 0.00513 ($p/T^\circ K$) must be added. These results agree very well with results from a gas mixing furnace (Hahn and Muan, 1960) and less well with vapor pressure measurements (Ingraham, 1966; Kim *et al.*, 1966; Shenouda and Aziz, 1967; Otto, 1964).

The reaction between bixbyite, pyrolusite, and vapor has been investigated by many workers, but the results disagree. The literature has been ably reviewed by Otto (1965). Few investigators have claimed that their reaction reached equilibrium, and none have

TABLE 1. SELECTED MANGANESE OXIDE BUFFER DATA

Buffer	Equation[a] for $\log f_{O_2}$	Source
Bixbyite-pyrolusite	$10.97 \ - \dfrac{8850}{T} + 0.0190 \left(\dfrac{p}{T}\right)$	Mah (1960)
Hausmannite-bixbyite	$7.896 - \dfrac{9848}{T} + 0.00513\left(\dfrac{p}{T}\right)$	Huebner and Sato (1968)
Manganosite-hausmannite	$13.42 \ - \dfrac{25715}{T} + 0.0807 \left(\dfrac{p}{T}\right)$	Huebner and Sato (1968)
Manganese-manganosite	$7.431 - \dfrac{40057}{T} + 0.0622 \left(\dfrac{p}{T}\right)$	Mah (1960)

[a] T in $^\circ K$, p in atm.

characterized their MnO_2 phase (crystal structure, composition, grain size and surface area). Because of the divergence of experimental data, the bixbyite-pyrolusite buffer was calculated from thermochemical data (Mah, 1960), resulting in the equation

$$\log f_{O_2} = 10.97 - \frac{8850}{T^\circ K} + 0.0190 \left(\frac{p}{T}\right) \qquad (7)$$

Equations for the manganese oxide buffer reactions selected for use in the present investigation, and for the manganese-manganosite buffer, are summarized in Table 1. The relative positions of oxygen buffers in the systems Fe-O, Mn-O, Ni-O, and C-O may be compared with the aid of Figure 3. The pattern of buffer curves for the system Mn-O is greatly expanded when compared to the Fe-O system buffers, reflecting the great stability of the Mn^{2+} ion. Manganosite has a much larger stability field than wustite because the manganese oxide is more stable than wustite. The hausmannite and magnetite fields are of comparable size, but the hausmannite field is displaced toward more oxidizing conditions. The bixbyite field is relatively small due to the appearance of pyrolusite at high f_{O_2} values.

Experimental results[1]

Runs on the graphite buffer:

Equilibrium of the assemblage rhodochrosite, manganosite, graphite,

and gas is well established at 960, 1480, and 1974 atm total pressure. At 960 atm the equilibrium decomposition temperature of rhodochrosite is 703 ± 5°C. A run at 705.5°C developed carbonate rims (about manganosite grains mixed with the graphite buffer) at the cooler end of the capsule (toward the head nut) but significant carbonate was not formed in the buffer at the other end. The charge was not appreciably decomposed. The decomposition is bracketed by runs at 700.5°C ($MnCO_3$ stable) and 706.5°C (MnO stable). At 1480 and 1974 atm, equilibrium decomposition temperatures at 746 ± 6° and 773 ± 5°C, respectively.

Runs on the nickel-nickel oxide buffer:

Carbonate was grown and decomposed along the Ni-NiO buffer at total pressures of 960 and 1974 atm. An outer charge of unannealed rhodochrosite was placed between the buffer and inner charge capsule (containing $MnCO_3$ or MnO) to prevent nickel from entering the charge. X-ray powder diffraction diagrams of carbonate and manganosite charges from the Ni-NiO runs are the same as those on the manganese oxide or graphite buffers. Equilibrium rhodochrosite decomposition occurs at 708 ± 5°C and 960 atm and at 777.5 ± 3° and 1974 atm.

Runs on the manganosite-hausmannite buffer:

The f_{o_2} of the mangenosite-hausmannite buffer lies above that of the bomb material (approximately the f_{o_2} of the Ni-NiO buffer) as is shown by the reduction of hausmannite to manganosite at the ends of the outer capsule where the buffer is exposed to the bomb atmosphere. The buffer immediately surrounding the charge is not reduced. Equilibrium decomposition of rhodochrosite is at 704.5 ± 6°C and 960 atm, 748 ± 9° and 1480 atm, and 778 ± 5° and 1974 atm.

Runs on the hausmannite-bixbyite buffer:

The equilibrium temperature of rhodochrosite decomposition to an oxide along the hausmannite-bixbyite buffer could not be determined with as great a certainty as with that for the graphite or manganosite-hausmannite buffers. Decomposition to hausmannite is very slow. The extreme sluggishness of the reaction is probably caused by the low temperatures and extremely small concentrations of O_2 and CO. The extent of this decomposition reaction at low temperatures is small. With the exception of the highest temperature runs in which hausmannite was identified in X-ray powder diffraction diagrams, run products were determined optically. Oxides formed reddish to black flakes in the charge, and the entire charge was discolored. Carbonate grew on both hausmannite and bixbyite grains, but was better developed around bixbyite grains. A drop of water added to the bomb in two runs (at 371°, 401°C)

catalyzed the carbonate growth. The added H_2O does not enter into the reaction; f_{CO_2} is depressed a small amount, but not enough to shift the rhodochrosite field boundary appreciably; f_{O_2}, internally buffered, remains unchanged. In these two runs, carbonate formed at lower f_{CO_2} values than if the run had been made in a dry atmosphere at the same pressure.

Care must be taken to raise the effective f_{O_2} of the bomb walls by permitting a layer of oxides to line the bomb well, or the buffer will be reduced to hausmannite or hausmannite+manganosite, and rhodochrosite will grow at anomalously high temperatures. Carbonate was observed to grow about the buffer grains at temperatures as high as 600°C in some initial runs. Generally, the buffer was more reduced towards the end of the capsule than at the center, demonstrating response to the more reducing bomb environment. Unless carbonate rims grew in the center of the buffer, adjacent to the charge capsule, a run was not accepted as indicating rhodochrosite stability.

The results of runs on the hausmannite-bixbyite buffer are plotted on Figures 6 and 7. Runs with water added to the charge give minimum temperatures. Several runs at higher temperatures are omitted. Decomposition of rhodochrosite occurs at 330°±23°C and 960/996 atm and at 430±35°C and 1974 atm. Even in runs lasting more than eight weeks, slow reaction rates do not permit a closer approach to the invariant point $MnCO_3$-Mn_3O_4-gas. Runs which showed no reaction in either direction have not been plotted on the figures but are listed in the table deposited with ASIS.

Runs on the bixbyite-pyrolusite buffer:

Runs on the bixbyite-pyrolusite buffer present problems similar to those of the runs on the hausmannite-bixbyite buffer. At temperatures higher than the rhodochrosite stability field, the charge became discolored (brown, gray, or black). In some cases, hausmannite was identified by X-ray powder diffraction. Few runs definitely indicated growth of rhodochrosite on the buffer grains. With transmitted light, opaque grains show halos of such intensity that they were mistaken for incipiently developed carbonate rims in some of the first runs.

Runs which showed discernible reaction are plotted in Figure 7. A colorless to pale brown, highly birefringent, fibrous, unidentified phase grew in several runs. The fibers are minute, approaching the limit of optical resolution. The high birefringence of this phase suggests that it may be a carbonate with an undescribed morphology.

The equilibrium decomposition temperature for rhodochrosite on the bixbyite-pyrolusite buffer is not well established. At 960 atm, hausmannite is a decomposition product in runs at 457°, 428°, and 381°C.

Four additional runs between 260.5° and 362°C show discoloration of the charge, interpreted as decomposition to bixbyite and/or hausmannite. Below 228°C, the carbonate charge remained unaltered. A trace of carbonate formed at 199°C. At 1974 atm., the charge became discolored in a run above 356°C; below 352°C the charge was unaltered, and in some cases carbonate formed in the buffer. Tentative equilibrium decomposition temperatures are 354° ± 20°C at 1974 atm and 230° ± 35°C at 960 atm.

The reaction $MnO + CO_2 = MnCO_3$:

Data for the rhodochrosite-manganosite-gas equilibrium are summarized in Table 2. Within the limits of experimental error, this reaction is independent of oxygen fugacity at constant total pressure. Isobaric sec-

TABLE 2. SUMMARY OF BUFFER INTERACTION FOR RHODOCHROSITE
DECOMPOSITION TO MANGANOSITE

Buffer	$p = 960$ atm	$p = 1480$ atm	$p = 1947$ atm
Graphite	703 ± 5[a] °C	746 ± 6	773 ± 5
Ni-NiO	708 ± 5		777.5 ± 3
"MnO"-Mn_3O_4	704.5 ± 6	748 ± 9	778 ± 5

[a] The uncertainty indicates the temperature gap between reversed runs, to which ± 3°C is added for uncertainties in temperature measurement, thermal gradient, etc.

tions at total pressures of 960, 1480, and 1974 atm are projected along the p axis in Figure 4. The change in f_{CO_2} as a function of f_{O_2} accounts for the curvature shown in the 1974 atm. section; as f_{O_2} decreases, f_{CO} increases, and f_{CO_2} decreases. The observed 5°C change between the MnO-Mn_3O_4 and the graphite buffers compares well with the calculated value of 6°C. At 960 atm the curvature is too slight to be detected experimentally. If equilibrium between graphite and gas did not prevail, the observed curvature would be too great (f_{O_2} below that calculated) or too little (f_{O_2} above that calculated for the graphite surface). The result that the rhodochrosite-manganosite-gas equilibrium is independent of the oxygen fugacity suggests that the manganosite composition is constant, if not stoichiometric, over the f_{O_2} range considered.

Data for the reaction manganosite + gas = rhodochrosite contained in Table 2, supplemented with data from the unbuffered runs by Goldsmith and Graf (1957), are plotted in Figure 5. All points have been plotted at a total pressure of 2000 atm, after correcting for the effect of pressure on the solid phases (Eugster and Wones, 1962; Orville and Greenwood, 1965). It was assumed that the molar volume change of the solids is
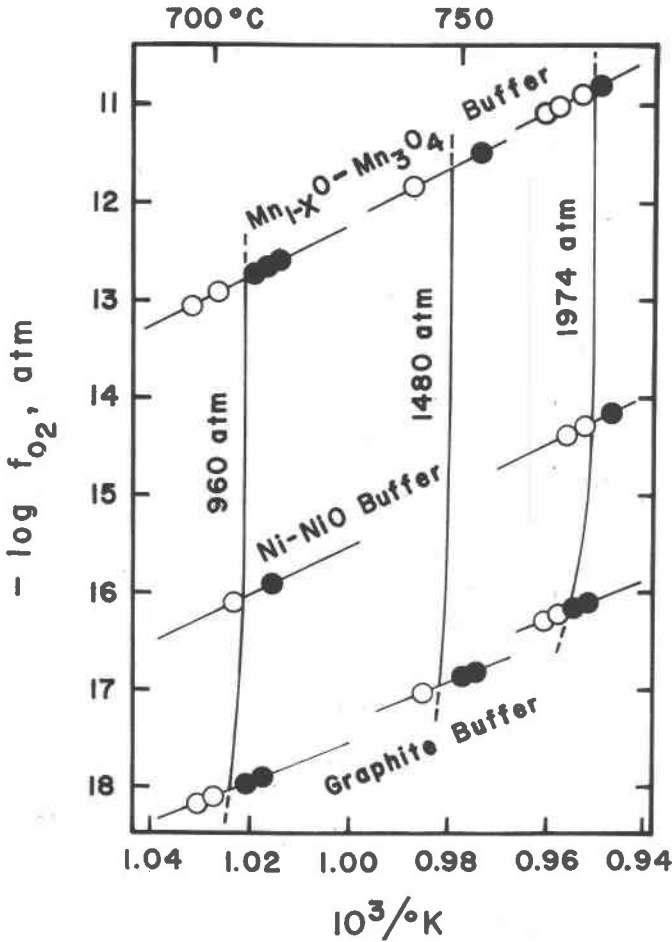
FIG. 4. Plots of selected runs positioning the isobaric f_{O_2}-T sections of the equilibrium surface rhodochrosite-manganosite-gas at 960, 1480, and 1974 atm projected along the pressure axis. Legend: open circle: rhodochrosite stable; solid circle: magnanosite stable.

17.84 cm³/mole for this reaction at all conditions investigated. Data obtained on the graphite buffer are corrected for the presence of CO and plotted for $p = 2000$ atm $= p_{CO_2}$. The difference between the buffered and unbuffered runs is within experimental error.

The equation for the equilibrium surface rhodochrosite-manganosite-gas in p-T-f_{O_2} space, based upon all available data, is

$$\log f_{CO_2}(\text{atm}) = 8.662 - \frac{5556}{T} + 0.0944\left(\frac{p}{T}\right). \tag{8}$$
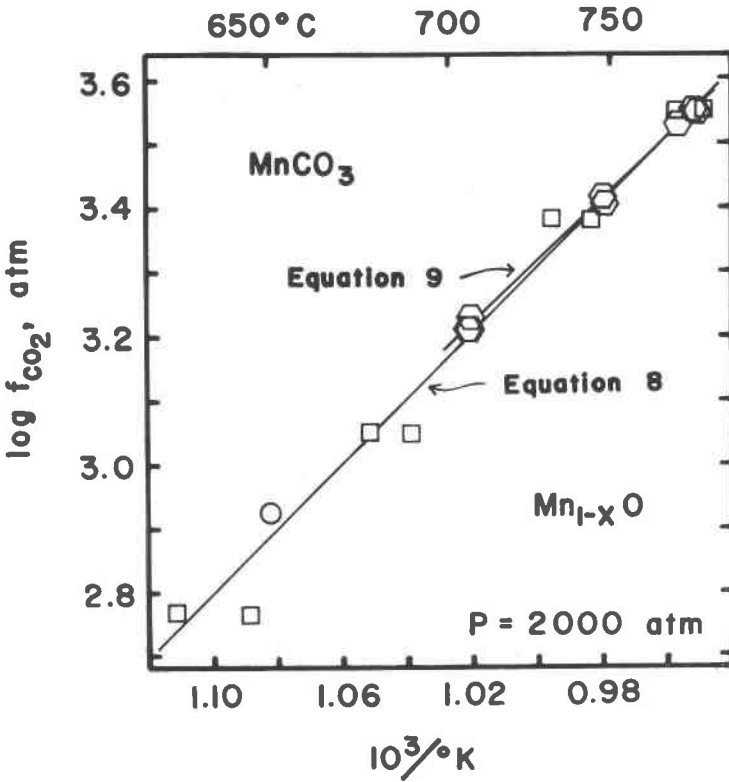
J. STEPHEN HUEBNER

Fɪɢ. 5. Data for rhodochrosite decomposition to manganosite. Graphite buffer points are corrected for the appreciable carbon monoxide present. All points corrected for 2000 atm. total pressure. Present investigation: Hexagon: Buffered reaction reversals; Open circle: Buffered run-rhodochrosite stable. Unbuffered runs of Goldsmith and Graf (1957): Bracketing squares.

Decomposition temperatures obtained in the present investigation yield the expression

$$\log f_{CO_2}(\text{atm}) = 8.040 - \frac{4910}{T} + 0.0944 \left(\frac{p}{T}\right). \tag{9}$$

Equation (8) is preferable to equation (9) in the sense that equation (8) is based on data that cover a wider temperature range than the data for the latter equation. However, the data by Goldsmith and Graf (1957) were based on runs of shorter duration and could not be duplicated by the present author when finely ground buffer was used.

The equilibrium constant of the reaction between manganosite, gas, and rhodochrosite is defined as

$$K = \frac{a_{MnCO_3}}{a_{Mn}f_{CO_2}} \tag{10}$$

The rhodochrosite composition does not deviate from pure $MnCO_3$, hence $a_{MnO_3} = 1$. In calculating the following thermodynamic values it was assumed that $a_{MnO} = 1$ and that the reaction proceeds as written in equation (2). At equilibrium, $\Delta G_{R_{298}} = \Delta G^\circ{}_{R_{298}} + RT \ln K = 0$ and log $K = -\log f_{CO_2}$. The enthalpy of reaction at one atmosphere total pressure based upon equation (8) is 25.4 kcal/mole and based upon equation (9) is 22.5 kcal/mole. The Goldsmith and Graf (1957) data yield 26.3 ± 1 kcal/mole (Robie, 1966), whereas the value calculated from the thermochemical data of Mah (1960) is 27.5 ± 1.7 kcal. The enthalpies of formation of manganosite and carbon dioxide (Mah, 1960) may be combined with the enthalpy of reaction to obtain the standard enthalpy of formation of rhodochrosite (Table 3). The literature values for $\Delta H^\circ f_{MnCO_3}$ (Mah, 1960; Moore, 1943) are 1 to 4 percent more negative than the experimental values; the manganosite composition, and the impurities in the natural sample used by Moore (1943) are possible sources of the discrepancy. Similarly the free energy of formation can be obtained for rhodochrosite (Table 4). Two sets of values for $\Delta H^\circ f_{MnCO_3}$ and $\Delta G^\circ f_{MnCO_3}$, based upon Equations 8 and 9, are tabulated in Tables 3 and 4. The differences between the two sets of values probably approximate the un-

TABLE 3. RHODOCHROSITE: ENTHALPY OF FORMATION FROM THE ELEMENTS[a]
(IN KCAL/MOLE AT 1 ATM PRESSURE)

Temperature, °K	ΔH_{MnCO_3} using equation (8)	ΔH_{MnCO_3} using equation (9)
298	−211.4	−208.6
400	−211.4	−208.5
500	−211.4	−208.4
600	−211.3	−208.4
700	−211.3	−208.4
800	−211.3	−208.4
900	−211.4	−208.5
1000[b]	−211.5	−208.6
1000	−212.9	−209.1
1100	−212.0	−209.1
1200	−212.1	−209.2

[a] $\Delta H_{MnCO_3} = \Delta H_{MnO} + \Delta H_{CO_{2(g)}} + \Delta H_{Reaction}$ Enthalpies of CO_2 and MnO are from Mah (1960). The enthalpy of reaction is from the present investigation and is based on Equations (8) and (9) as noted.

[b] Transition point, manganese.

TABLE 4. RHODOCHROSITE: FREE ENERGY OF FORMATION FROM THE OXIDES[a]
(IN KCAL/MOLE AT 1 ATM PRESSURE)

Temperature, °K.	Using equation (9)		Using equation (8)		Mah (1960)	Robie (1966)
	$\log K$	ΔG_{MnCO_3}	$\log K$	ΔG_{MnCO_3}	ΔG_{MnCO_3}	ΔG_{MnCO_3}
298	8.44	−11.50	9.98	−13.64	−14.45	−13.22
400	4.24	− 7.75	5.23	− 9.57	− 9.93	
500	1.78	− 4.07	2.45	− 5.61	− 5.45	
600	0.14	− 0.39	0.60	− 1.64	− 1.0	
700	−1.03	3.29	−0.72	2.32	3.35	
800	−1.90	6.96	−1.72	6.28		
900	−2.58	10.64	−2.49	10.25		
1000	−3.13	14.32	−3.11	14.21		

[a] For the reaction $MnO + CO_2 = MnCO_3$, $\log K = -\log f_{CO_2}$.

certainty in the thermochemical data derived from the results of these phase equilibria studies.

The reaction $6 MnCO_3 + O_2 = Mn_3O_4 + 6 CO_2$:

The results of the experimental investigation of this reaction are summarized in Figure 6. The buffers have been plotted as a function of log $K = \log (f_{CO_2}^6 / f_{O_2})$ and $1/T°K$. Runs on the hausmannite-bixbyite buffer have been plotted individually, but for the manganosite-hausmannite buffer, only the equilibrium decomposition temperatures (Table 2) are shown. The experimental results are not sufficiently precise to distinguish separate curves at 960 and 1974 atm; a single curve is drawn to fit the run data obtained at all values of total pressure. The equation of the experimentally determined curve is

$$\log K = 40.39 - \frac{9429}{T°K} + 0.486\left(\frac{p}{T}\right). \tag{11}$$

Values of log K for this reaction are calculated from thermochemical data and compared with the experimental values of Equation (11) in Table 5. Agreement between the experimentally determined and calculated values of log K is good in the temperature range of the experiments. Enthalpies of this reaction calculated from Equation (11) using the Clausius-Clapeyron equation and from tabulated thermochemical data are compared in Table 6. Agreement with a value calculated from Robie's (1966) data at 298°K is within the limits of uncertainty.

The reaction $4MnCO_3 + O_2 = 2Mn_2O_3 + 4CO_2$:

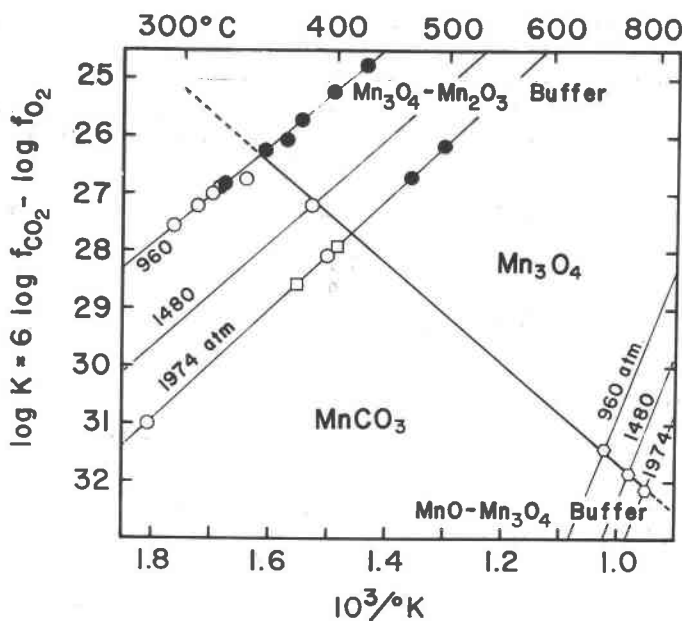Fig. 6. Data for the reaction $6 MnCO_3 + O_2 = 2 Mn_3O_4 + 6 CO_2$ plotted as a function of $\log K = 6 \log f_{CO_2} - \log f_{O_2}$ and $1/T °K$. Reaction reversals are plotted on the manganosite-hausmannite buffer; individual runs are positioned on the hausmannite-bixbyite buffer. The experimental data are not sufficiently precise to distinguish the change in $\log K$ for the rhodochrosite-hausmannite-gas equilibrium between 960 and at 1974 atm. Legend: Hexagon: Reversed reaction; Open circle: Rhodochrosite stable (dry); Open square: Rhodochrosite stable (H_2O added); Solid circle: Mn_3O_4 stable; Half solid circle: Both $MnCO_3$ and Mn_3O_4 formed.

TABLE 5. EQUILIBRIUM CONSTANT: RHODOCHROSITE-HAUSMANNITE-GAS REACTION
(1 ATM PRESSURE)[a]

$T.$, °K	From equation 11	Calculated from Mah (1960)	Calculated from Robie (1966)	Calculated with ΔG_{MnCO_3} from equation (8) combined with data from Mah (1960)
298	8.7	3.5	9.0	
600	24.7	24.1		22.6
700	26.9	26.8		24.8
800	28.6			26.4
900	29.9			27.8
1000	31.0			28.8

[a] $\log K = 6 \log f_{CO_2} - \log f_{O_2}$ for the reaction $6 MnCO_3 + O_2 = 2 Mn_3O_4 + 6 CO_2$.

TABLE 6. ENTHALPY OF REACTION[a]: RHODOCHROSITE-HAUSMANNITE-GAS EQUILIBRIUM (KCAL/MOLE, 1 ATM PRESSURE)

Temp., °K	Experimental slope of equation (11)	ΔH_{MnCO_3} based on equation (8)	ΔH_{MnCO_3} from Mah (1960)	ΔH_{MnCO_3} from Robie (1966)
298	43.1	41.8	56.5	47.2±6
400		41.6	56.0	
500		41.9	54.8	
600	43.1	41.9	53.3	
700	43.1	42.2	51.8	
800	43.1	42.5		
900	43.1	42.7		
1000[b]	43.1	43.0		
1000		45.8		
1100		42.9		

[a] $\Delta H_R = 6\Delta H_{CO_2} + 2\Delta H_{Mn_3O_4} - 6\Delta H_{MnCO_3} - \Delta H_{O_2}(gas)$.

[b] Transition point of manganese.

The reaction involving rhodochrosite, bixbyite, and vapor is not well positioned by the present investigation. Runs involving the bixbyite-pyrolusite buffer are unsatisfactory; reaction rates are very slow, an unidentified phase is present in some runs, and there were indications that equilibrium between the buffer and atmosphere may not have been obtained. Experiments pertinent to this reaction are plotted in Figure 7. The experimentally determined heat of reaction, 54 kcal. (from the data plotted in Fig. 7), does not agree with the thermochemical values in the literature. At 1974 atm the $MnCO_3$-Mn_2O_3-gas curve intersects the Mn_2O_3-MnO_2 buffer curve at about 354°C, giving an incorrect sequence of curves about the invariant point $MnCO_3$-Mn_3O_4-Mn_2O_3-gas (all three metastable extensions extend into the rhodochrosite+gas field). Either the temperature of rhodochrosite decomposition to oxide is placed at too high a value, or the Mn_2O_3-MnO_2 and Mn_3O_4-Mn_2O_3 buffer curves must be moved closer together. In view of the initial difficulties of establishing equilibrium between the buffer and the atmosphere, it is suggested that the inconsistent result is due to failure of the buffer, charge, and gas to equilibrate during the run, giving an erroneously high temperature of decomposition of $MnCO_3$.

The reaction $2 MnCO_3 + O_2 = 2 MnO_2 + 2 CO_2$:

The equilibrium between rhodochrosite, pyrolusite, and vapor was not determined in this investigation; no attempt was made to specify an oxygen fugacity above that of the Mn_2O_3-MnO_2 buffer. The curve for this reaction intersects that of the Mn_2O_3-MnO_2 buffer at 230°±35C and 960

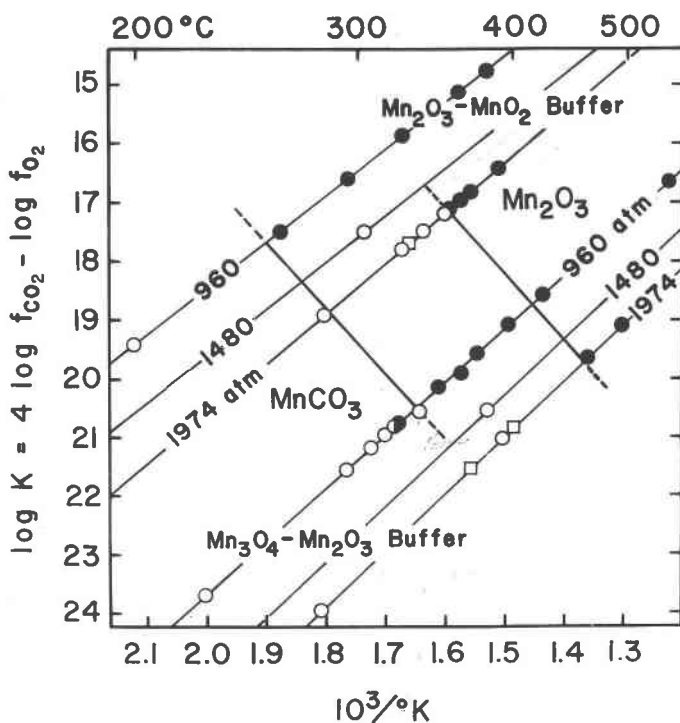FIG. 7. Experiments used in determining the reaction $4\ MnCO_3+O_2=2\ Mn_2O_3+4\ CO_2$. Runs are positioned on the buffer curves; buffers are plotted as a function of $\log K=4\ \log f_{CO_2}-\log f_{O_2}$ and $1/T°K$. Suggested reaction curves at 960 and 1974 atm. are shown. Legend: Open circle: Rhodochrosite stable; Open square: Rhodochrosite stable (H_2O added); Solid circle: Rhodochrosite decomposed; Half-solid circle: Rhodochrosite discolored and carbonate growth in buffer.

atm and at $354°\pm 20°$C and 1974 atm; the uncertainty of the locations of these points is largely due to experimental difficulties. Experimental and calculated values of log K are in satisfactory agreement. This reaction is positioned on Figure 8a by calculating the enthalpy of reaction (9 to 12 kcal; Mah, 1960; Robie, 1966) and constructing a surface with appropriate slope through the temperatures of buffer intersection (Figures 8a, b).

Comparison of experimental and calculated rhodochrosite stability fields:

The experimental and calculated rhodochrosite stability fields are best compared with the aid of isobaric f_{O_2}-T sections, Figures 8a and 8b. Agreement between the experimental and calculated manganosite-hausmannite and hausmannite-bixbyite buffer curves is not good. The experimental buffer curves selected for use in this investigation define a larger
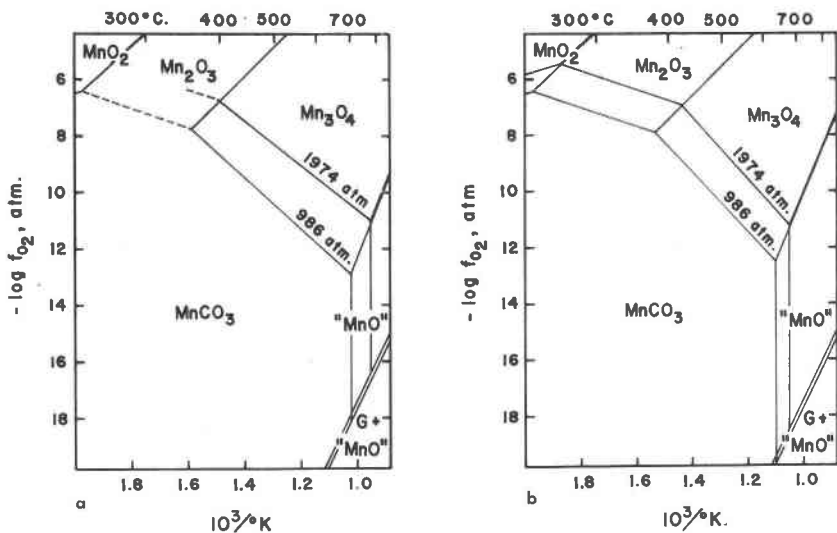
FIG. 8. Rhodochrosite stability field at 986 and 1974 atm (a) as determined in this investigation. The buffer curves are based on experiments at higher temperatures or are calculated from thermochemical data, as discussed in the text. The equilibria rhodochrosite-manganosite-gas and rhodochrosite-hausmannite-gas are calculated from Equations (8), (9), and (11). Decomposition along the Mn_2O_3-MnO_2 buffer at 986 atm is tentatively positioned at $230 \pm 35°C$. $MnCO_3$-MnO_2-gas is calculated to pass through the isobarically invariant point $MnCO_3$-Mn_2O_3-MnO_2-gas at 230°C and 986 atm. (b) by thermodynamic calculations based on the data of Mah (1960). The graphite-vapor buffer is from French and Eugster (1965). At temperatures greater than 700°K, the free energy of rhodochrosite was extrapolated from values at lower temperatures.

field for hausmannite and a smaller field for bixbyite, than the calculated curves.

The rhodochrosite field has been calculated using data from Mah (1960). The experimentally determined reaction rhodochrosite-manganosite-gas does not agree well with the calculated values. At the temperatures considered, a small error in free energy of reaction causes a relatively large error in the calculated decomposition temperature. The experimentally determined equilibrium curves for the rhodochrosite to hausmannite+gas reaction agree better with calculated curves based upon the data by Mah. The tentative experimental data for the reaction rhodochrosite to bixbyite+gas at 960 atm agree best with data from Mah. The curve for the rhodochrosite-pyrolusite-gas equilibrium is based on calculations. Calculations combining the rhodochrosite thermochemical data derived from this study with the oxide data of Mah (1960) do not agree with the experimentally determined $MnCO_3$ field. At best these

thermochemical calculations indicate an internal consistency among the data for rhodochrosite, hausmannite, and bixbyite. The thermochemical data for the manganese oxides must be reappraised.

DISCUSSION

The position and shape of the rhodochrosite stability field in p-T-f_{O_2} space accounts for the natural rhodochrosite-manganese oxide assemblages. Manganosite is a rare mineral because it is stable only when temperature is high relative to carbon dioxide fugacity (at an f_{O_2} value within the manganosite field). Manganosite is expected to form only by the decarbonation of rhodochrosite or reduction of hausmannite. Syngenetic precipitation of manganese monoxide is improbable because, in addition to the requirement of low f_{O_2} (within the manganosite field), the f_{CO_2} must be smaller than about 10^{-8} (Equations 8, 9). Most known occurrences of manganosite have formed by the decomposition of carbonate (Magnusson, 1930; Watanabe, 1959; Epprecht, 1946).

The assemblage rhodochrosite-hausmannite has been described by many investigators; excepting the metamorphic manganese oxide ores of India, hausmannite is commonly accompanied by the manganese carbonate. At the Buckeye mine and the Smith prospect, California (Huebner, 1967) and at the Casalas mine, France (Perseil, 1965), hausmannite forms small (to several tenths of a millimeter) idioblasts in xenoblastic rhodochrosite; at the Buckeye mine such rhodochrosite is nearly pure $MnCO_3$. Hausmannite has locally replaced carbonate; there has been grain-boundary equilibrium between the oxide and carbonate.

The strong f_{O_2}-T dependence of the rhodochrosite-hausmannite-gas equilibrium makes the occurrence of rhodochrosite-hausmannite relatively common. This assemblage coexists with manganosite at high temperatures, but it also forms at lower temperatures and higher oxygen fugacities, more commonly achieved during the metamorphism of manganese deposits.

The equilibrium association of rhodochrosite with bixbyite is unknown. At temperatures prevailing during metamorphism and within the range of oxygen fugacity which covers the bixbyite field, improbably high f_{CO_2} values are required for rhodochrosite stability. Similar reasoning applies to the explanation of the absence of the equilibrium assemblage rhodochrosite-pyrolusite in nature. The presence of bixbyite or pyrolusite indicates that the oxygen fugacity was too high for the formation of rhodochrosite at geologically reasonable values of T, p, and f_{CO_2}.

Quadrivalent manganese oxides, here represented by pyrolusite, are observed to precipitate from thermal waters at the earth's surface (Hewett and Fleischer, 1960) under conditions of low pressure and tem-

perature, and at an f_{O_2} of about 0.2 atm. Rhodochrosite is not stable under these conditions. Rhodochrosite precipitation requires more reducing conditions, such as those which prevail in a fissure filled with hydrothermal fluid or a restricted ocean basin.

The diagram of the rhodochrosite stability field, Figure 8a, indicates the stable mineral assemblages in the system Mn-C-O. A comparison of natural assemblages described in the literature with the stable assemblages shown on the diagram immediately shows that certain apparently incompatible associations exist in nature. The association of graphite with hausmannite, as at the Merid mine, Brazil (Horen, 1953), is an example. Impossibly high pressures are required to cause the graphite-gas surface to cross the manganosite field and intersect the hausmannite field. The equilibrium association of graphite and bixbyite is also not possible in the earth's crust. The association of graphite with any manganese oxide except manganosite is evidence for disequilibrium. Graphite-manganosite and graphite-rhodochrosite assemblages are permissible. Careful search may reveal these heretofore unreported assemblages.

The presence of pyrolusite or bixbyite in an ore implies metamorphic conditions under which the oxygen fugacity is higher than in graphite- or magnetite-bearing metasedimentary and meta-igneous rocks. Within some rocks, syngenetic manganese dioxides, represented by pyrolusite, have been metamorphosed to bixbyite or hausmannite, indicating a loss of oxygen. Such systems must have been "open" to O_2. Steep oxygen chemical potential gradients must have existed between bixbyite ores and surrounding graphite- or magnetite-bearing country rocks. At 527°C and 2000 atm total pressure, for example, the minimum $\log f_{O_2}$ for bixbyite stability is -4.4, whereas the magnetite-hematite assemblage is stable at $\log f_{O_2} = -17$. Rocks adjacent to the manganese ore bodies should be examined for evidence of iron oxidation.

Metamorphism of a syngenetic manganese oxide deposit commonly involves reduction and a loss of oxygen. The associated values of f_{O_2} are too great for the crystallization of rhodochrosite at all but impossibly high f_{CO_2} values. Furthermore, f_{CO_2} is likely to be low in an oxide body devoid of primary carbonate, and the common siliceous country rocks cannot supply the CO_2 needed for this reaction. Conversely, the metamorphism of a rhodochrosite body is not likely to result in assemblages with bixbyite or pyrolusite because oxygen must be added in such reactions. The surrounding rocks, with an f_{O_2} less than that required for the formation of bixbyite or pyrolusite, cannot act as an oxygen reservoir or source. This crude model may be used to evaluate the extent to which syngenetic manganese ores tend to retain their original characteristics during metamorphism. Syngenetic oxide bodies may be reduced during metamor-

phism, but tend to yield oxides; syngenetic rhodochrosite bodies are meta-morphosed to recrystallized rhodochrosite, and perhaps rhodochrosite+manganosite by decarbonation, but higher oxides are not formed. Many rhodochrosite-hausmannite deposits probably recrystallized isochemi-cally with only mutual local replacement of mixed syngenetic rhodochro-site and manganese oxide.

Naturally occurring rhodochrosite commonly deviates from end member composition (see, for instance, Wayland, 1942; Deer *et al.*, 1962). Carbonates approximating the rhodochrosite composition are less com-mon than manganiferous calcium, magnesium, and iron carbonates. The results of the present investigation can be used to predict the effect of the $MnCO_3$ component on the stability fields of calcite, magnesite, and sider-ite (Figure 9). This discussion must remain qualitative in the absence of thermodynamic data on the nonideal behavior of carbonate solutions.

At 2000 atm CO_2 pressure, pure calcite decomposes at about 1300°C. (Harker and Tuttle, 1955). Goldsmith and Graf (1957) report that the decarbonation temperature is greatly decreased by the addition of man-ganese. Calculations based on their data suggest that the activity co-efficient of $MnCO_3$ exceeds 1.80 for certain solution compositions. The
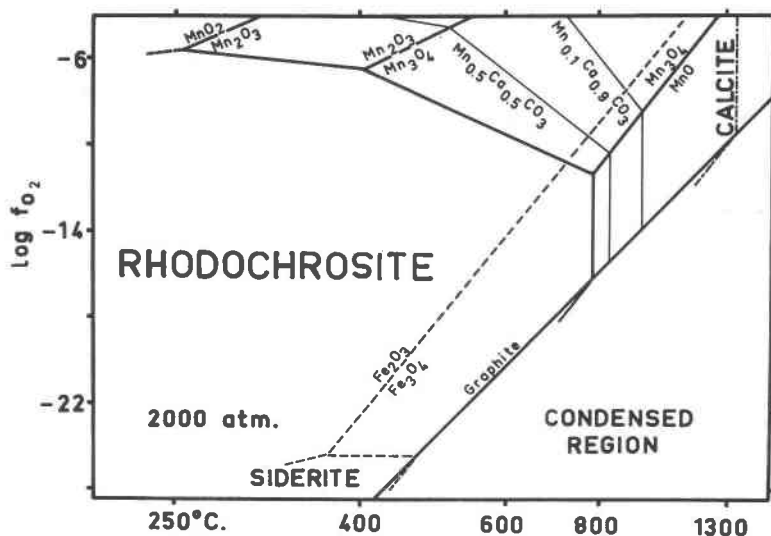

FIG. 9. T-f_{O_2} section at 2000 atm showing the stability fields of rhodochrosite, siderite, and calcite. Data for rhodochrosite are taken from the present investigation. The rhodo-chrosite stability field extends to much higher temperatures and oxidizing conditions than the siderite field. Calcite decomposition to portlandite occurs at high temperatures, but if manganese is present, the decomposition results in the progressive depletion of the $MnCO_3$ component to form MnO and a more calcium-rich carbonate.

calculations of activity are not sufficiently precise to calculate the decomposition of rhodochrosite-calcite solid solutions to hausmannite and bixbyite; these relations are sketched in Figure 9. The stability field of a manganiferous carbonate is a function of f_{O_2}, in addition to T, p, and f_{CO_2}.

The addition of manganese to magnesite will not appreciably change the magnesite stability within the manganosite field because the p_{CO_2}-T curves for the simple decarbonation of the two carbonates are very similar (Goldsmith, 1959). At f_{O_2} values above the manganosite field, the temperature of decomposition of rhodochrosite-magnesite solid solution to hausmannite or bixbyite decreases with increasing f_{O_2}.

The decomposition of siderite (French, 1964) occurs at markedly lower temperatures and oxygen fugacities than that of rhodochrosite. The addition of bivalent manganese to siderite will increase the carbonate stability field. Although the phase relations of the intermediate oxides are not well known, possible carbonate decomposition products include Fe-Mn spinel solid solution, hausmannite solid solution, hematite solid solution, bixbyite solid solution, and manganosite-wustite solid solution. Manganese in solid solution in iron oxide buffers will raise the f_{O_2} values defined by these buffers because the oxidation potentials of the manganese oxide buffers are greater than those of the corresponding iron oxide buffers. Siderite cannot decompose to wustite or iron at 2000 atm in the presence of gas because the magnetite field extends to lower f_{O_2} values than the siderite field or the graphite-vapor surface at these pressures. Beneath the graphite surface carbon dioxide is reduced to graphite.

REFERENCES

AMINOFF, G. (1926) Über die Kristallstruktur von Hausmannite (MnMn$_2$O$_4$). *Z. Kristallogr.*, **64,** 475–490.

BLUMENTHAL, R. N., AND D. H. WHITMORE (1961) Electrochemical measurements of elevated-temperature thermodynamic properties of certain iron and manganese oxide mixtures. *J. Amer. Ceram. Soc.*, **44,** 508–512.

BRICKER, OWEN P. (1965) Some stability relations in the system Mn-O$_2$-H$_2$O at 25°C and one atmosphere total pressure. *Amer. Mineral.*, **50,** 1296–1354.

BURNHAM, CHARLES W. (1962) Lattice constant refinement. *Carnegie Inst. Wash. Year Book*, **61,** 132–135.

DAVIES, M. W., AND F. D. RICHARDSON (1959) The nonstoichiometry of manganous oxide. *Trans. Faraday Soc.*, **55**, 604–610.

DEER, W. A., R. A. HOWIE, AND J. ZUSSMAN (1962) *Rock-forming minerals. V. 5 Non-silicates.* John Wiley and Sons, Inc., New York, 371 p.

EPPRECHT, W. VON (1946) Die Manganmineralien vom Gonzen und ihre Paragenese. *Schweizer. Mineralog. Petrog. Mitt.*, **26**, 19–27.

ERNST, W. G. (1966) Synthesis and stability relations of ferrotremolite. *Amer. J. Sci.*, **264**, 37–76.

EUGSTER, H. P., AND D. R. WONES (1962) Stability relations of the ferruginous biotite, annite. *J. Petrology*, **3**, 82–125.

FEITKNECHT, W. (1964) Einfluss der Teilchengrösse auf den Mechanismus von Festkörper-reaktionen. *Pure Appl. Chem.*, **9**, 423–440.

FINCH, G. I., A. P. B. SINHA, AND K. P. SINHA (1957) Crystal distortion in ferrite-man-ganites. *Proc. Roy. Soc. (London) Ser A*, **242**, 28–35.

FOSTER, P. K., AND A. J. E. WELCH (1956) Metal oxide solid solutions: I. Lattice constants and phase relationships in ferrous oxide (wustite) and in solid solutions of ferrous oxide and manganous oxide. *Trans. Faraday Soc.*, **52**, 1626–1635.

FRENCH, B. M. (1964) *Stability of Siderite and Progressive Metamorphism of Iron Forma-tion.* Ph.D. Thesis, The Johns Hopkins University, Baltimore, Maryland, 357 p.

———— AND H. P. EUGSTER (1965) Experimental control of oxygen fugacities by graphite-gas equilibriums. *J. Geophy. Res.*, **70**, 1529–1539.

————, AND P. ROSENBERG (1965) Siderite ($FeCO_3$): Thermal decomposition in equilib-rium with graphite. *Science*, **147**, 1283–1284.

GELLER, S., J. A. CAPE, R. W. GRANT, AND G. P. ESPINOSA (1967) Distortion in the crystal structure of α-Mn_2O_3. *Phys. Lett.*, **24A**, 369–371.

GILBERT, M. C. (1966) Synthesis and stability relations of the hornblende ferropargasite. *Amer. J. Sci.*, **264**, 698–742.

GLASSER, F. P. (1962) The ternary ststem CaO-MnO-SiO_2. *J. Amer. Ceram. Soc.*, **45**, 242–249.

GOLDSMITH, J. R. (1959) Some aspects of the geochemistry of carbonates, *In* P. H. Abelson, ed., *Researches in Geochemistry*, John Wiley and Sons, Inc., New York, 336–358.

———— (1960) Subsolidus relations in the system $CaCO_3$-$MgCO_3$-$MnCO_3$. *J. Geol.*, **68**, 324–335.

————, AND D. L. GRAF (1957) The system CaO-MnO-CO_2: solid solution and decomposi-tion relations. *Geochim. Cosmochim. Acta*, **11**, 310–334.

GRAF, D. L. (1961) Crystallographic tables for the rhombohedral carbonates. *Amer. Mineral.*, **46**, 1283–1316.

HAHN, W. C., JR., AND A. MUAN (1960) Studies in the system Mn-O: the Mn_2O_3-Mn_3O_4 and Mn_3O_4-MnO equilibria. *Amer. J. Sci.*, **258**, 66–78.

HARKER, R. I., AND O. F. TUTTLE (1955) Studies in the system CaO-MgO-CO_2. Part 2: Limits of solid solution along the binary join $CaCO_3$-$MgCO_3$. *Amer. J. Sci.*, **253**, 274–282.

HED, A. Z., AND D. S. TANNHAUSER (1967) Contribution to the Mn-O phase diagram at high temperature. *J. Electrochem. Soc.*, **114**, 314–318.

HEWETT, D. F., AND MICHAEL FLEISCHER (1960) Deposits of the manganese oxides. *Econ. Geol.*, **55**, 1–55.

HOCHGESCHWENDER, K. AND T. R. INGRAHAM (1967) Use of thermal conductivity gas analysis for thermodynamic measurements on the dissociation of CuO, Mn_2O_3 and MnO_2. *Can. Metall. Quart.*, **6**, 71–84.

HOREN, A. (1953) *The Manganese Mineralization at the Merid Mine, Minas Gerais, Brazil.* Ph.D. Thesis, Harvard University, Cambridge, Massachusetts.

HUEBNER, J. S. (1967) *Stability Relations of Minerals in the System Mn-Si-C-O.* Ph.D. Thesis, The Johns Hopkins University, Baltimore, Maryland, 279 p.

HUEBNER, J. S., AND M. SATO (1968) Determination of the equilibrium oxygen fugacities of the manganese oxides. (abstr.) *Trans. Amer. Geophys. Union,* **49,** 342.

INGRAHAM, T. R. (1966) Thermodynamics of the Mn-S-O system between 1000°K and 1250°K. *Can. Metall. Quart.,* **5,** 109–122.

ISIHARA, T., AND A. KIGOSHI (1953) Fundamental researches on the metallurgical treatment of manganese ores. I: On equilibrium in the reduction of Mn_3O_4 with CO. *Tohoku Univ. Sci. Rep. (Sendai) Ser. A,* **5,** 172–178.

JAY, A. H., AND K. W. ANDREWS (1945) Note on oxide systems pertaining to steelmaking furnace slags. FeO-MnO, FeO-MgO, CaO-MnO, MgO-MnO. *J. Iron Steel Inst. (London),* **152,** 15p–18p.

KIM, D. Q., Y. WILBERT, AND F. MARION (1966) Sur la determination directe des equilibres des oxydes de manganese a haute temperature. *Compt. Rend. Acad. Sci. Paris, Ser. C.,* **262,** 756–758.

KLINGSBERG, C., AND R. ROY (1960) Solid-solid and solid-vapor reactions and a new phase in the system Mn-O. *J. Amer. Ceram. Soc.,* **43,** 620–626.

KRAUSKOPF, K. B. (1957) Separation of manganese from iron in sedimentary processes. *Geochim. Cosmochim. Acta,* **12,** 61–84.

KUBASCHEWSKI, O., AND E. L. EVANS (1958) *Metallurgical Thermochemistry.* Pergamon Press, London. 426 p.

LE BLANC, M., AND G. WEHNER (1934) Beitrag zur Kenntnis der Manganoxyde. *Z. Phys. Chem.,* **168A,** 59–78.

LINDSLEY, D. H. (1963) Fe-Ti oxides in rocks as thermometers and oxygen barometers. *Carnegie Inst. Wash. Year Book,* **62,** 60–66.

MAGNUSSON, N. H. (1930) Langbans Malmtrakt. *Sver. Geol. Undersokn. Ser. Ca,* **23,** 111 p.

MAH, ALLA D. (1960) Thermodynamic properties of manganese and its compounds. *U. S. Bur. Mines, Rep. Invest.,* **5600,** 34 p.

MASON, B. (1943) Mineralogical aspects of the system $FeO-Fe_2O_3-MnO-Mn_2O_3$. *Geol. Foren. Stockholm Forh.,* **65,** 97–180.

——— (1944) The system $Fe_2O_3-Mn_2O_3$: Some comments on the names bixbyite, sitaparite, and partridgeite. *Amer. Mineral.,* **29,** 66–69.

McMURDIE, H. R., B. M. SULLIVAN, AND F. A. MAUER (1950) High temperature X-ray study of the system $Fe_3O_4-Mn_3O_4$. *J. Res. U. S. Nat. Bur. Stand.,* **45,** 34–41.

MOORE, G. E. (1943) Heat content of manganese dioxide and carbonate at high temperature. *J. Amer. Chem. Soc.,* **65,** 1398–1399.

MOORE, T. E., M. ELLIS, AND P. W. SELWOOD (1950) Solid oxides and hydroxides of manganese. *J. Amer. Chem. Soc.,* **72,** 856–866.

ORVILLE, P. M., AND H. J. GREENWOOD (1965) Determination of ΔH of reaction from experimental pressure-temperature curves. *Amer. J. Sci.,* **263,** 678–683.

OSWALD, H. R., AND M. J. WAMPETICH (1967) Die Kristallstrukturen von Mn_5O_8 und $Cd_2Mn_3O_8$. *Helvetica Chim. Acta,* **50,** 2023–2036.

OTTO, E. M. (1964) Equilibrium pressures of oxygen over $Mn_2O_3-Mn_3O_4$ at various temperatures. *J. Electrochem. Soc.,* **111,** 88–92.

——— (1965) Equilibrium pressures of oxygen over $MnO_2-Mn_2O_3$ at various temperatures. *J. Electrochem. Soc.,* **112,** 367–370.

PALACHE, C., H. BERMAN, AND C. FRONDEL (1944) *The system of Mineralogy. vol. 1.* John Wiley and Sons, Inc., New York, 834 p.

PERSEIL, A. (1965) Association de braunite et hausmannite dans un niveau manganesifere de Casalas (Ariege). *Bull. Soc. Franc. Mineral. Cristallogr.*, 88, 300–303.

PETTERSON, H. (1946) Investigation of solubility relations in the solid state in the binary systems of the oxides CaO, MnO, MgO, and FeO. *Jernkontorets Ann.*, 130, 653–663.

RIBOUD, P. V., AND A. MUAN (1962) Phase equilibria in a part of the system "FeO"-MnO-SiO$_2$. *Trans. AIME*, 224, 27–33.

——— (1963) Melting relations of CaO-manganese oxide and MgO-manganese oxide mixtures in air. *J. Amer. Ceram. Soc.*, 46, 33–36.

ROBIE, R. A. (1966) Thermodynamic properties of minerals, *Geol. Soc. Amer. Mem.*, 97, 437–458.

———, P. M. BETHKE, M. S. TOULMIN, AND J. L. EDWARDS (1966) X-ray crystallographic data, densities, and molar volumes of minerals. *Geol. Soc. Amer., Mem.*, 97, 27–73.

RODE, E. YA (1949) Physicochemical study of manganese oxides. *Izvest. Sektora Fiz.-Khim. Anal., Inst. Obshchei i Neorg. Khim., Akad. Nauk SSSR*, 19, 58–68. [*Chem. Abstr.*, 44, 9228 (1950)].

ROSENBERG, P. E. (1963) Synthetic solid solutions in the systems MgCO$_3$-FeCO$_3$ and MnCO$_3$-FeCO$_3$. *Amer. Mineral.*, 48, 1396–1400.

SCHWERDTFEGER, K., AND A. MUAN (1967) Equilibria in the system Fe-Mn-O involving "(Fe, Mn)O" and (Fe, Mn)$_3$O$_4$ solid solutions. *Trans. AIME*, 239, 1114–1119.

SHENOUDA, F., AND S. AZIZ (1967) Equilibria and hysteresis in the system Mn$_2$O$_3$-Mn$_3$O$_4$-O$_2$. *J. Appl. Chem.*, 17, 258–262.

SOUTHARD, J. C., AND C. H. SHOMATE (1942) Heat of formation and high-temperature heat content of manganous oxide and manganous sulfate. High-temperature heat content of manganese. *J. Amer. Chem. Soc.*, 64, 1770–1774.

SWANSON, H. E., N. T. GILFRICH, AND M. I. COOK (1957) Standard X-ray diffraction powder patterns. *U. S. Nat. Bur. Stand. Circ.*, 539(7), 70.

TUTTLE, O. F. (1948) A new hydrothermal quenching apparatus. *Amer. J. Sci.*, 246, 628–635.

——— (1949) Two pressure vessels for silicate-water studies. *Geol. Soc. Amer. Bull.*, 60, 1727–1729.

ULRICH, K-H., K. BOHNENKAMP, AND H. J. ENGELL (1966) Über die Gleichgewichte von Magnetit-Hausmannit-Mischkristallen mit Wustit-Mangen(II)oxid-Mischkristallen und Sauerstoff und die Reduktion von Magnetit-Hausmannit-Mischoxiden. *Z. Phys. Chemie*, 51, 35–49.

VAN HOOK, H. J., AND M. L. KEITH (1958) The system Fe$_3$O$_4$-Mn$_3$O$_4$. *Amer. Mineral.*, 43, 69–83.

VERWEY, E. J. W., AND J. H. DE BOER (1936) Cation arrangement in a few oxides with crystal structures of the spinel type. *Rec. Trav. Chim.*, 55, 531–540.

WATANABE, T. (1959) The minerals of the Noda-Tamagawa mine, Iwate Prefecture, Japan. *Mineral. J. (Tokyo)*, 2, 408–421.

WAYLAND, R. G. (1942) Composition, specific gravity, and refractive indices of rhodochrosite; rhodochrosite from Butte, Montana. *Amer. Mineral.*, 27, 614–628.

WEIDNER, J. R., AND O. F. TUTTLE (1965) Stability of siderite, FeCO$_3$. (abstr.) *Geol. Soc. Amer., Spec. Pap.*, 82, 220.